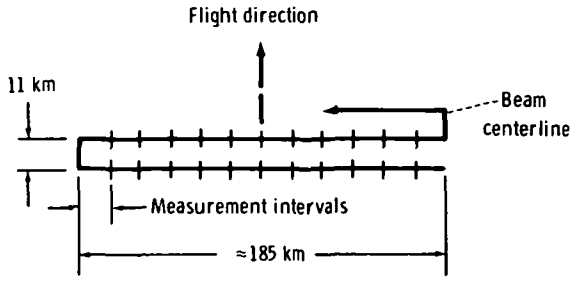

FIGURE 5–81.—The CTC mode.

are needed in the reliability of the antenna gimbaling, switching logic, and polarization isolation. System drifts, resolution, and noise-level fluctuations have to be reduced in future airborne and spaceborne systems.

Data-processing techniques: For operational systems, highly efficient data-processing techniques are needed; no reliable data-display techniques have been advanced to date. Onboard processing of data should be explored, and the digitally processed data should be color coded to display ocean winds and waves for visual interpretation and use. These programs should be capable of handling large volumes of reflectivity data and displaying these data on a world map.

Calibration data measurements: For spaceborne and airborne instruments, the calibration data corresponding to each subsystem are usually measured in the laboratory. The amplifier, mixer, and filter gains are some examples. For instruments flown for extended periods, these internal gains change. To alleviate this problem, automatic calibration modes should be designed to check all calibration data needed to calculate backscattering cross sections from raw data.

Applicability.—Multifrequency, multipolarization scatterometers can be used to measure winds and waves at the surface of the ocean and to detect development and progress of storms. These surface measurements can be used to predict weather and to forecast storm developments. Sea-state forecasting will aid in the navigation and routing of ships.

SUBSURFACE SOUNDERS

This section is concerned with airborne or spaceborne electromagnetic systems used to detect subsurface features.

The skin depth of a wave propagating into the ground, defined as the depth at which the electromagnetic field decays to e^{-1} of its value at the surface, is given by

$$\delta = \left(\frac{2\rho}{\mu_0 \omega}\right)^{1/2} \qquad (5\text{–}36)$$

where ρ is resistivity of the ground material (ohm-m), μ_0 is magnetic permeability of free space (H/m), ω is angular frequency $=2\pi f$, and f is frequency of the electromagnetic wave (Hz). Resistivities for normal ground rank between 10 ohm-m for clay soil to 3000 ohm-m for gravel and rock (ref. 5–23). To sound such ground to any appreciable depth, very low frequency (vlf) will have to be used. At 10 kHz, a skin depth of approximately 15 m will result for a ground with a 10-ohm-m resistivity, for example. With a resistivity of 1000 ohm-m, the corresponding skin depth is 150 m. At a frequency of 100 MHz, the skin depths are 0.15 and 1.5 m for the same resistivities.

The resistivities vary with the content of water and with the temperature. In permafrost regions, the ice contained in the ground may cause resistivities of approximately 100 000 ohm-m.

Radio-Wave Method

Soundings at a vlf with active devices are impractical because of interference from radio transmitters with signals that are propagated over very long distances along the surface of the Earth. However, one may take advantage of these vlf signals for investigation of subsurface features by using the so-called wave-tilt method. At a given position at the ground (fig. 5–83), the vertically polarized radio surface wave radiated from a vlf station may be resolved into the three components shown. The ratio between the longitudinal and the vertical electrical components is the wave tilt, which is dependent on the resistivity of the ground.

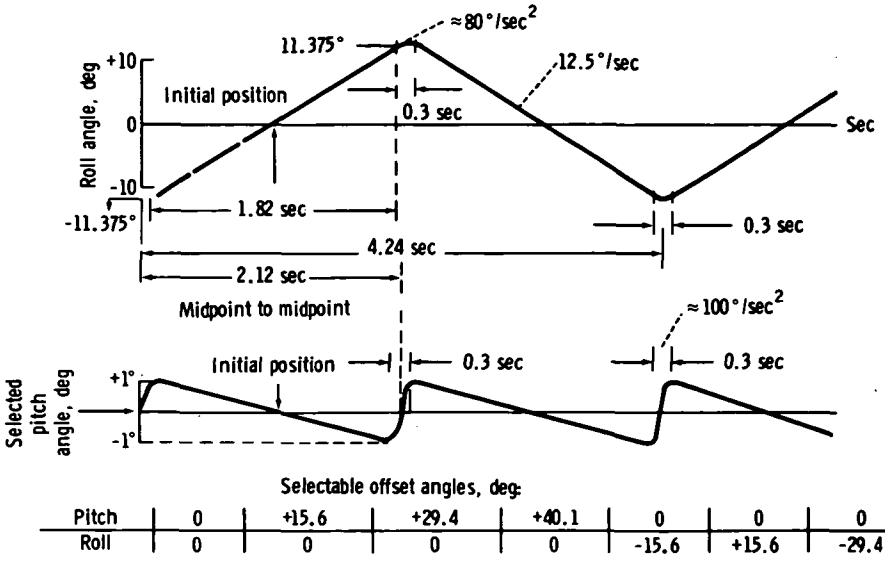

Selectable offset angles, deg:

Pitch	0	+15.6	+29.4	+40.1	0	0	0	0
Roll	0	0	0	0	-15.6	+15.6	-29.4	+29.4

Scan-measurement pattern:

Twelve measurement periods (M1 to M12) of 151.5 msec each. The same measurement sequence in each.
Beam center roll motion per measurement = 1.896°.

Measurement 151.5 msec		Total beam center angular measurement excursion = 22.75°											
		M1	M2	M3	M4	M5	M6	M7	M8	M9	M10	M11	M12
Beam center motion = K x 1.896°	From: K =	±6	±5	±4	±3	±2	±1	0	±1	±2	±3	±4	±5
	To: K =	±5	±4	±3	±2	±1	0	±1	±2	±3	±4	±5	±6

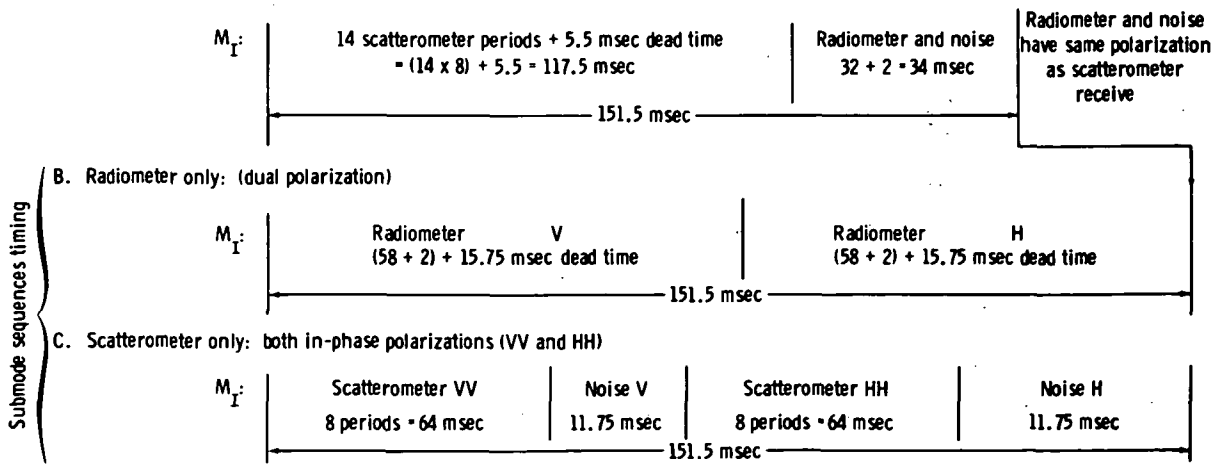

FIGURE 5-82.—Measurement sequences for the CTC mode.

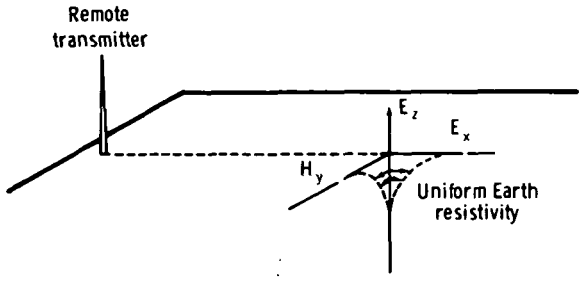

FIGURE 5–83.—Electromagnetic field components of a vertically polarized radio surface wave.

If the ground consists of layers of different resistivity, which will be penetrated by the radio wave, the layering will be reflected in the wave tilt. In simple cases in which the ground consists of two or three horizontal layers, the inverse problem may be solved eventually by using the signals from two radio stations.

Measurements may be carried out at ground level with a dipole that can be turned about a horizontal axis so that the actual wave tilt (approximately a few degrees from vertical) may be determined. Measurements may also be conducted from a low-flying aircraft using the so-called E-phase system. This system is based on the fact that the wave tilt $W=E_x/E_z$ has equal in-phase and quadrature-phase components. The E_x and E_z components are measured with two short dipole antennas, one horizontal and one vertical. Aircraft roll causes leakage of E_z into the horizontal antenna, but this signal is in phase. Therefore, by measuring the quadrature-phase component of W, errors caused by leakage are avoided.

The airborne measurements are conducted by flying approximately 60 m above the ground. The wave tilt is a local effect; that is, when passing a boundary between two regions with different resistivity, the wave tilt changes almost abruptly when measured at ground level. At heights over the ground, an "integration" effect occurs so that the change in wave tilt is smoothed out. To obtain a good resolution, the measuring height should be as low as possible. A resolution of approximately 25 m is obtained when measured at a height of approximately 60 m over the terrain.

In an existing system, the various signals of importance for computing the wave tilt, as well as an altimeter signal, are recorded on analog and magnetic tape recorders operated during the flight along lines in the terrain. A flightpath camera eases identification of the data relative to existing maps. Data reduction is conducted after completion of the flights.

The method of wave-tilt measurement based on the in-phase and the quadrature-phase components is valid only if conductive currents in the ground dominate over displacement currents; that is, low-resistivity ground. When conductive currents are not dominant, the true sensitivity can often be computed, although this computation requires some knowledge of the ground.

Two-Antenna Method

Another method of measuring the ground resistivity, which is the reciprocal of the conductivity, is to measure the change in coupling between two antennas caused by the influence of the ground.

The two antennas are small loops (magnetic dipoles) mounted 3 m apart in each end of a dielectric rod. The rod is held parallel to the ground with the loops at 45° to horizontal. One loop is used for transmitting and the other for reception at a low frequency. Far from the ground, the coupling signal between the two antennas is phased out. At low heights over the ground, the transmitted signal causes currents in the conductive ground, and these currents produce a signal at the receiver output. The conductance of the ground directly under the horizontal rod can be determined by computation.

In principle, the conductivity of two horizontal layers may be determined by measurements at more than one frequency. The measurements are conducted from a helicopter; to avoid the influence of the helicopter, the antenna rod is extended far under the vehicle. The height of the rod over the ground should be as low as feasible—60 m,

for example—because this technique also is relying on a local effect. The resolution is approximately 25 m and is of particular application for conducting ore detection.

Radio Echo Sounding

Because of the interference problem, sounding at a vlf, which permits penetration to appreciable depths, seems impractical. At vhf, that is, at frequencies above 30 MHz, the interference problem may be of minor importance in remote areas, but the absorption in the ground is very large; therefore, only moderate depths are reached. For example, at 100 MHz, silty clay soil with a water content of 15 percent (weight) gives an absorption of 2.5 dBm (ref. 5–24); thus, a system with a large system sensitivity (ratio between transmitted power and minimum detectable power) is required to reach appreciable depths. With an existing pulse radar system, a layer with a reflection coefficient of −10 dB should be observable at a depth of approximately 20 m. However, the reflection of the surface is, in this case, large (−3.5 dB); therefore, the received surface pulse becomes very large and tends to saturate the receiver so that near-surface reflecting interfaces may not be detectable.

The radio echo sounding method seems useful for detection of reflecting interfaces only in special cases over ground with small losses. Examples are polar ice (i.e., glaciers in polar regions and the inland ice in Greenland and Antarctica), areas of permafrost (although presence of unfrozen water may give high attenuation), some desert areas (except in cases where the content of salt is appreciable), and lunar soil and rock.

Simple radar systems have been designed for radio echo sounding of polar ice at several frequencies below 500 MHz. The systems rely on the facts that the absorption in the ice is very low (0.02 dBm at 253 K) and that the radio wave velocity V is independent of the ice temperature (until 273.25 K) and pressure ($V=169$ m/μsec, since $\epsilon=3.2$). The systems are used for airborne measurement of the thickness of icecaps and for detection of stratifications in the ice, which establish horizons in the ice and give information about the flow pattern of ice.

Typical airborne systems operate at 60 and 300 MHz and are flown simultaneously 300 to 1000 m over the surface of the ice (ref. 5–25). The principle of the measuring system is shown in figure 5–84, which illustrates a standard pulse radar system with a dipole antenna array mounted under the wing of the aircraft. The received echoes are displayed on an A-scope (real presentation of the video signal) and on a Z-scope (intensity modulated presentation). Both oscilloscopes are photographed, the A-scope intermittently and the Z-scope by a continuous moving film. The latter gives continuous profiles for each flight line. For position identification, the films are supplied with time marks that relate to marks on the recording of the inertial navigation data.

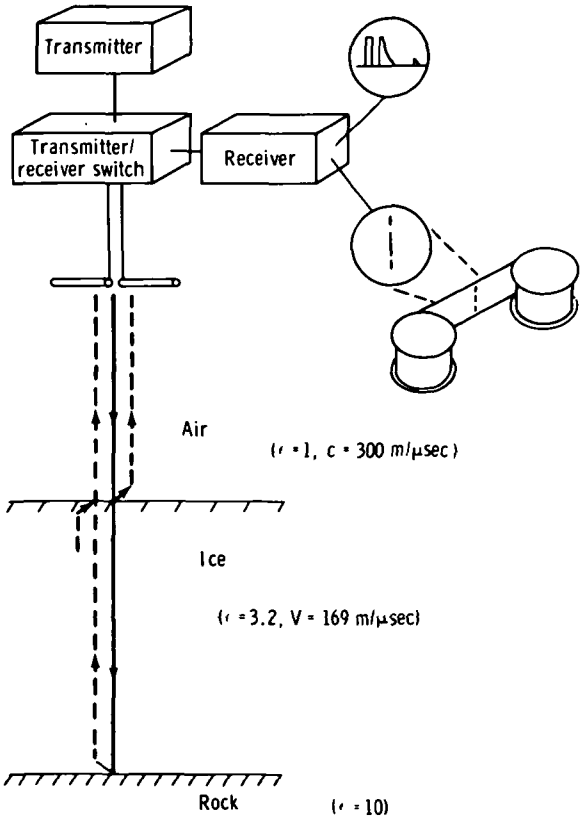

FIGURE 5–84.—Operational diagram of a radio echo sounder.

The system at 60 MHz is able to detect bedrock echoes in the greater part of the ice sheets in Greenland and Antarctica; that is, through more than 4500 m of ice. Stratification echoes have been detected down to approximately 3000 m below the surface, but this performance is dependent on the ice temperature (losses are temperature dependent). The vertical resolution relies on the pulse width. With the shortest pulse (60 μsec), a resolution of 6 m is obtained. In areas with thick ice in which the total absorption is large, a wide pulse (1 μsec) and corresponding narrow bandwidth (1 MHz) are used, giving a resolution of 100 m. In the other directions, the resolution is determined with the antenna radiation pattern. At 60 MHz, the antenna is a linear array of four dipoles mounted transverse to the flight direction. Therefore, good resolution is obtained transverse to the flight direction, whereas the longitudinal resolution is relatively poor, although refraction effects in the surface improve the situation. Because of the large radiation fore and aft, the bedrock features are generally represented by hyperbolas. A computer technique exists to correct for this effect. At 300 MHz, this effect virtually does not exist because a rectangular array of four dipole (backfire) antennas is used. However, this system is less sensitive and is designed for measurement over shallow ice only.

An improved version of ice-sounding radar is presently being tested. With an increase of the system sensitivity (increased transmitter power) and an introduction of a pulse compression technique, a vertical resolution of approximately 10 m should be obtained at all depths.

In several instances, the attempt has been made to sound temperate glaciers and ice sheets with the same technique. So far, these attempts have been unsuccessful because of scattering from a multitude of water inclusions in the glaciers. In polar ice, crevasses and ice lenses cause a similar effect.

The Apollo 17 lunar sounder system has been flown on both the Earth and Moon. This sounder system relies on direct reflection from surface and subsurface interfaces (as the previously mentioned system).

The system uses frequencies at 150, 15, and 5 MHz, which were chosen for various depths and resolutions of sounding of lunar rocks and soils in which electromagnetic waves are much less attenuated than in similar Earth materials. At all frequencies, the SAR technique is used, which gives a large dynamic range and low side lobes. A functional diagram is shown in figure 5–85 (ref. 5–26). The figure illustrates how along-track resolution ρ_x is obtained, despite the wide regular beamwidth of the antennas, by using a coherent radar (i.e., one in which both transmitter and receiver are phase referenced to a stable master oscillator) in conjunction with data storage and processing. A given terrain element of range R is observed by the radar while moving along a track subtended

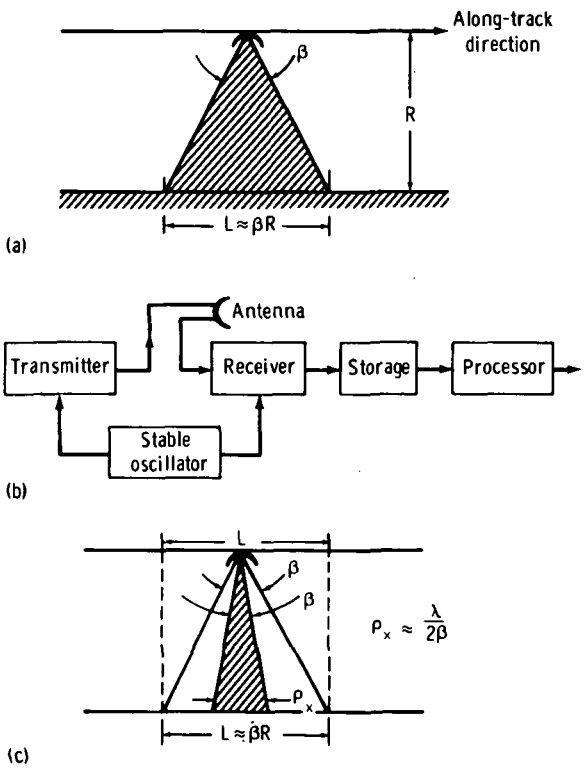

FIGURE 5–85.—Functional diagram of the Apollo 17 lunar sounder system SAR. (*a*) Physical beamwidth. (*b*) Simplified block diagram. (*c*) Improved along-track resolution ρ_x.

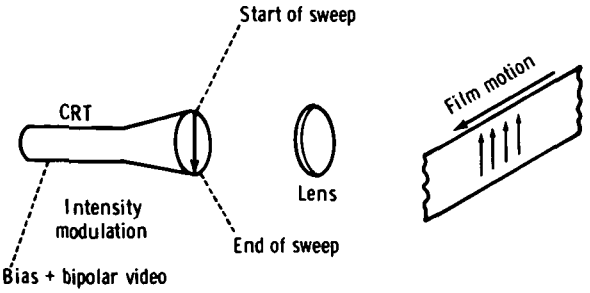

FIGURE 5–86.—Simplified diagram of the lunar sounder system SAR optical recorder.

by an angle β. Stored data collected during the observation time and processed to synthesize an antenna aperture of length L yield the improved along-track resolution ρ_x.

Systems parameters, such as system bandwidth and time-bandwidth product of the transmitted signal, are chosen so that the range/depth resolution is proportional to wavelength. At 5 MHz, a free-space resolution of 700 m is obtained. The resolution in the surface material will be finer given by ρ_x/n, where n is the refractive index. The along-track resolution in free space is obtained by the synthetic aperture technique to be 5λ, or 300 m at 5 MHz.

The video outputs of the radar systems are recorded (stored) on a CRT film-type optical recorder with all signals on the same 70-mm film, the 150-MHz system having a bandwidth of 16 MHz (fig. 5–86). This film is later processed on the ground in a coherent optical system (fig. 5–87) to perform the necessary along-track and/or range-processing operation. This processor is equipped

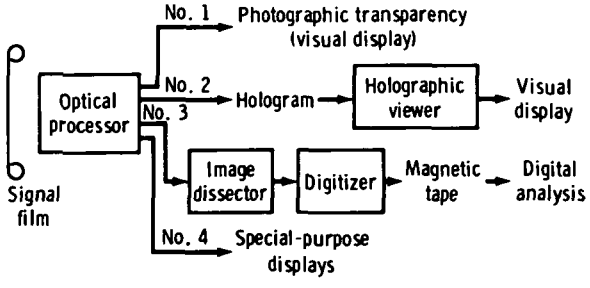

FIGURE 5–87.—The lunar sounder system SAR basic processor/display system.

with several alternate readouts, including a photographic hardcopy, a hologram, and a digital tape.

A prototype was flown at approximately 10 km above the Earth. Penetration in the Greenland ice cap was observed at 150 MHz, and a series of layers was recorded down to approximately 140 m, the limitation in depth being the result of the small power available (95-W peak). A combination of the features of the two sounders mentioned here may result in a system that may be used from low-orbit satellites to sound polar ice sheets and glaciers.

The 2-m mode of the lunar sounder can be used for an image of the ocean and solid-Earth surface from nadir to approximately 30 km. A distorted "cylinder perspective" image strip is obtained, with an average resolution of approximately 5λ. The prototype was used to obtain images of wave crests on the ocean, which showed the spacing and orientation of the crests.

The antenna patterns of the lunar sounder have very wide angular beamwidths (ref. 5–26); therefore, the system can be used as a scatterometer (ref. 5–27). The wide angular beamwidth gives the system the capability to receive reflected energy from small regions over wide angles in both the crosstrack and along-track directions. The measurement of reflection vis-a-vis angle is precisely the purpose of a scatterometer (ref. 5–18). Using an optical setup to focus (or position) the range in the same plane as the Doppler spectrum is obtained, the amount of reflection from any location within an angular beamwidth can be found (ref. 5–27). The resolution of the system used as a scatterometer is identical to that of focused SAR in the range direction (an inverse function of the bandwidth and approximately 5λ). In the Doppler direction, the half-power resolution is that of unfocused SAR ($[(\lambda R)/2]^{\frac{1}{2}}$, where R is range). From an altitude of 10 km, this resolution is approximately 150 m for the 2-m sounder mode. These resolutions compare favorably with those of a conventional scatterometer.

Experiment Application for a Subsurface Sounder

This section outlines an example of one experimental approach to detect the presence and determine the location of subsurface geological structures from an aircraft. The sensor used would be capable of performing large-area surveys of subsurface Earth resources, such as subsurface water tables, mineral deposits, oil location, and geological structure formation for mining purposes.

Prior development.—Electromagnetic subsurface sounding with active radio instrumentation has been used successfully in the geophysical exploration for groundwater and mineral deposits. Most sounding systems are CW that use at most a few frequencies. More recent developments use a pulse transient approach, which is still a variation on CW exploration (ref. 5–28). Both techniques have been operated on the ground or from low-flying aircraft, with the depth of exploration from 100 to 400 m. The techniques rely on a simple, anomaly/no-anomaly decision or on model fitting for interpretation. In the latter instance, the types of realistic geological models that can be computed are limited, and a large question of uniqueness exists in the interpretation. Two obvious areas of improvement in state of the art are greater depth of exploration and a more direct means of interpreting data. A time-delay approach, analogous to active seismic exploration for oil, is an attractive method for improving the means of interpretation. However, it has been thought that the frequency range needed for significant penetration, in typical geological materials, is in the kilohertz range. In this frequency band, dispersion is so great at bandwidths required for adequate resolution that a time-delay scheme is not practical (ref. 5–29). A notable exception to the previous discussion is Antarctic ice sounding (ref. 5–25), which operates successfully in the high-frequency (hf) region (35 MHz–8 m) because of the low loss tangent (and thus also low dispersion) of the ice. A second exception is lunar material (because of the complete absence of water) as was demonstrated by the Apollo 17 deep sounding lunar experiment.

This section describes a time-delay system that will operate in a wide range of geological materials and to depths greater than have been achieved from previous airborne instruments. This instrument operates in the hf range (100 kHz to 10 MHz) to avoid significant dispersion in materials with conductivities as high as 10^{-2} $(\text{ohm-m})^{-1}$ or loss tangents as high as 1.0.

Observed phenomena.—The previously mentioned experiment uses radar techniques to observe the discontinuities in dielectric constant on and within the surface layer of the Earth. From the phase information in the echo and the time-delay or equivalent frequency shift, the nature of the dielectric discontinuity and its location can be inferred. The analysis includes computer ray-tracking techniques and iterative techniques for establishing the depth of the subsurface feature. The detection of the presence of a subsurface discontinuity is unambiguous. The location determination depends on knowledge about the dielectric constant of the intervening material. Thus, the uncertainty in depth varies as the square root of the uncertainty in the dielectric constant. Most Earth subsurface materials in their natural state (the type with loss tangents less than 0.5) in the hf range (100 kHz to 10 MHz) have a dielectric constant between 9 and 16. Hence, the maximum likely uncertainty is 14 percent. The typical depth of penetration varies with the loss tangent of the intervening layers. A diagram that indicates typical performance is given in figure 5–88.

Experiment technique.—The experiment approach uses coherent radar techniques at long wavelengths and records the echoes on an optical recorder. (These measurements could be performed from an aircraft.) The basic technique uses the long-frequency sweep (used by FM altimeters) and the coherent format to increase the average effective power radiated to a level at which the successful observation of the subsurface features is highly probable. The combination

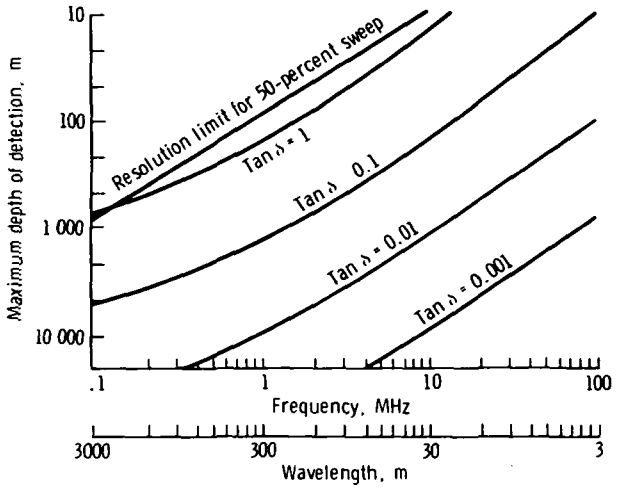

FIGURE 5–88.—Maximum depth of penetration and resolution as a function of frequency for various loss tangents, where tan δ is loss tangent.

of the coherent radar, the long linear FM sweep, and the optical recorder are the new aspects of this sounder.

The linear sweep and a typical response are characterized in figure 5–89. The apparatus consists of a linear sweep generator,

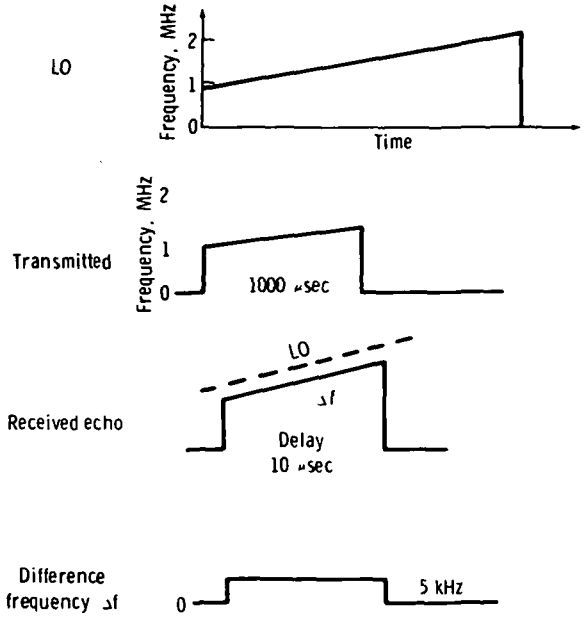

FIGURE 5–89.—Diagrams of typical frequency compared to time for the long-wavelength sounding radar.

transmitter, antenna, and receiver. The video output from the receiver is recorded on film by an optical recorder. The film is then processed by an optical correlator to produce an image film that is digitized, processed, and used to print out the subsurface feature locations.

The antenna consists of a deployable reel-type unit mounted in the tail of an aircraft. The maximum length is variable from 300 to 30 m. The matching of the transmitter to the antenna to minimize ringing or range side-lobe levels poses one of the most difficult problems associated with this experiment.

Once the instrument is installed on the aircraft, flights must be at relatively low altitudes over areas where conditions favor detection of known subsurface features. The preliminary data-acquisition flights may be used to verify the sounder performance and data reduction and interpretation techniques. One such area is the Chuckwalls Valley, which is northeast of Salton Sea in southern California.

The system operates over a 50-percent bandwidth; that is, 100 to 150 kHz or 2 to 3 MHz. The system is tunable in discrete steps over the range from 100 kHz to 10 MHz. The choice of frequency depends on the depth of penetration desired, the loss in the material, and the resolution required. The antenna is a deployable reel-type unit, and the antenna length may be adjusted as needed to operate at the highest possible efficiency.

System performance.—The system presented is an adaptation of FM altimeter radar techniques to low frequencies for use in a sounding mode. The transmitted frequency is a repetitive linear ramp of long duration. The transmitted frequency also serves as the reference frequency; sweep bandwidth must be kept high to attain adequate resolution. However, because the received frequency is mixed with a replica of the transmitted frequency and the sweep rate is slow, the system achieves significant bandwidth reduction to improve the signal-to-noise ratio with no appreciable loss in range

resolution. During data processing, a further bandwidth reduction may be attained to select returns from directions normal to the flightpath, such as pools of water beneath the aircraft. This technique is also known as Doppler filtering.

If the transmitted waveform has a frequency that sweeps over a total bandwidth B in an interval of T seconds, the frequency of a return delayed by Δt seconds will be $f_s = B\,\Delta t/T$.

The signal return has a duration of T seconds, and if it is passed through a filter of bandwidth $1/T$ at a center frequency f_s, then a return that has a delay of Δt with a total uncertainty of $1/B$ will pass through this filter. The noise bandwidth is also $1/T$; thus, a reduction of noise power by $1/TB$ may be achievable. This effect is equivalent to the time bandwidth product TB signal-to-noise ratio improvement that can be obtained with a conventional chirp pulse-compression system, but the system is not limited by dispersed pulse length compatible with round-trip delay time to the first surface.

The resolution is equivalent to

$$\Delta R = \frac{c}{2B\sqrt{\epsilon}} \qquad (5\text{–}37)$$

where c is velocity of light and ϵ is dielectric constant, which is essentially limited only by the total bandwidth sweep of the system.

The maximum depth of exploration for an ideal system without Doppler filtering has been computed on the following basis. The return power from a first surface of reflectivity γ_1 at a range R is given by

$$P_r = \frac{P_t G^2 \gamma_1 N \lambda_0^2}{(4\pi)^2 (2R)^2} \qquad (5\text{–}38)$$

where P_t is transmitted power, G is antenna pattern gain, N is antenna efficiency, and λ_0 is radio wavelength in free space. Equation (5–39) gives the return power from a subsurface layer located at a depth d in a medium for which the loss tangent is $\tan \delta$:

$$P_r = \frac{P_t G^2 N \lambda_0^2 (1-\gamma_1)^2 \gamma_2 L_1}{(4\pi)^2 (2R)^2} \qquad (5\text{–}39)$$

where γ_2 is the subsurface reflection coefficient and L_1 is the material loss. The loss in the material is given by

$$L_1 = 10^{-5.48 \tan \delta\, \epsilon_1^{1/2}\, d/\lambda_0} \qquad (5\text{–}40)$$

where ϵ_1 is dielectric constant. The expected noise comes primarily from sources outside the antenna. The noise power may be expressed by

$$P_n = kT_a BN \qquad (5\text{–}41)$$

where k is Boltzmann constant, T_a is ambient noise temperature, B is noise bandwidth of the system, and N is antenna efficiency. The expected ambient noise temperature T_a caused by manmade noise in rural environments follows the following relationship within 10 dB from quiet areas to noisy areas:

$$T_a = \frac{3 \times 10^7}{f^{2.5}} \qquad (5\text{–}42)$$

where the frequency f is in megahertz.

System parameters used to calculate the performance curves in figure 5–88 are as follows:

1. Peak power: 10 W
2. System bandwidth: 0.5 f (f=carrier frequency)
3. Noise bandwidth: 1000 Hz
4. Frequency sweep duration: 1 msec
5. Antenna efficiency: 0.01
6. First surface dielectric: 10 to 15 (ref. 5–30)
7. Second surface dielectric: 2 (oil)

Engineering development.—Airborne radar-sounding systems have demonstrated the ability to detect dielectric discontinuities beneath glaciers. The problem of designing a sounding radar instrument to detect discontinuities below moist Earth materials is more complex because the propagation loss of radio waves is greater in these materials than in ice. Increasing the peak radiated power can only alleviate this problem to a certain extent at the expense of a more cumbersome instrument. Operation at lower altitudes restricts the transmitted energy because the transmitted pulse length must not exceed the minimum round-trip elapsed time of the radio wave. The technique discussed would

circumvent this problem by using a technique that has been previously used at much shorter radio wavelengths in radio altimetry. With this technique, reception is simultaneous with transmission, and the waveform separation is accomplished by an instantaneous frequency separation of the transmitted frequency from the received frequency. This technique requires some unique characteristics of portions of the sounding radar for proper operation.

Description.—The sounding radar system shown in the functional diagram (fig. 5–90) consists of a sweeping LO, a low-noise power amplifier, an antenna, and a high-level mixer. The LO generates a linear frequency sweep that is amplified by a low-noise power amplifier, and this power is radiated by the antenna. The return signal is coupled from the transmitter-antenna line by a directional coupler into a high-level mixer. The return signal is then mixed with the transmit waveform. The output of the mixer is a waveform for which the frequency is directly proportional to the range of the reflecting surface. The output of this mixer is passed through a high-pass filter and amplified before recording in an optical recorder. The data stored in the optical recorder film are processed by taking a two-dimensional transform of the data film in an optical processor, filtering through a narrow-pass spatial filter in azimuth, and recording in an output data film. The result is an image for which the dimensions are along-track distance and cross-track distance (depth of discontinuity).

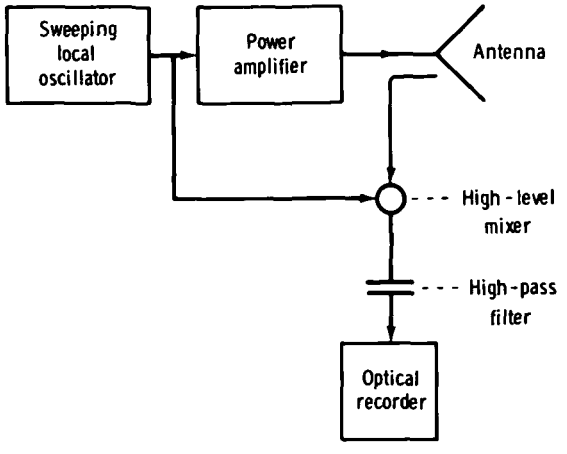

FIGURE 5–90.—Functional diagram of sounding radar system.

DOPPLER FILTERING AND MOVING TARGET INDICATOR

Some radar applications mentioned in earlier chapters have required some form of Doppler filtering or moving-target indicator (MTI) to determine the velocities or velocity spread of targets such as precipitation or ocean waves. Doppler radar provides information on the relative velocity between the targets and the radar; the information can be derived from many types of radar waveforms by using coherent processing.

The simplest form of Doppler radar involves pure CW transmissions. The returned signal spectrum is broadened by the Doppler spectrum of target movements, and the spectrum will be shifted in frequency when the radar is located on a moving platform. For CW transmissions, the desired spectrum will be contaminated by the Doppler spectrum of unwanted returns from land/sea. The width of this unwanted spectrum is set by the basic line width of the radar coherent reference convolved with the Doppler spread of groundspeed seen by the radar beam shape. For large dynamic range requirements, the Doppler spectrum seen by side lobes may also be significant and may set a limit on side-lobe levels. The Doppler resolution is therefore determined by this spectrum of unwanted clutter; and, for CW transmission, this can only be improved by reduction of antenna beamwidth and side-lobe levels.

For most applications, Doppler processing is combined with ranging, which enables range gating to be used to exclude (or reduce) unwanted responses outside the principal region of interest. As with SAR, coherent signal processing is necessary. This will entail either coherent transmissions or storage of phase information on each transmitted pulse referred to a stable LO (coherent-on-receive). The basic limit on Doppler resolution is set by the stability

(spectral line width) of the phase reference over the integration period of the radar. This limit will be further degraded by the Doppler spectrum from moving clutter such as returns from the surface of the Earth.

Discrimination and analysis of the Doppler return are performed by filtering the bipolar video waveform. The MTI techniques require the use of a high-pass filter response. Such a system rejects targets at or near the reference Doppler frequency, as conditioned by the filter response, but there is no classification of target velocities. The information relating to the relative speed between the radar and the ground can often be extracted from an appropriate range gate to provide a "clutter-locked" reference.

Doppler classification of targets within a range cell requires the use of multiple bandpass filtering (or digital fast-Fourier-transform (FFT) techniques) for each cell of interest. This technique is pulse Doppler or range-gate filtering and can lead to a very large number of filters (or associated digital storage) when targets may exist at any range. The storage is proportional to the product of the number of range cells and Doppler filters for a given dynamic range. The frequency response of the bandpass filtering is also repeated at multiples of the PRF.

The main limitation on measuring target velocity from a satellite or aircraft-borne radar wil be the residue of this unwanted spectrum from side lobes in range and azimuth. The problems of seeing slow-speed targets such as precipitation near the surface of the Earth can place severe constraints on the design of large narrow-beam antennas with low side lobes.

Traffic moving along a road in England seen from an aircraft-mounted, side-looking radar incorporating MTI processing is shown in figure 5–91. The corresponding radar map without MTI processing is shown for comparison.

In principle, the raw radar data from a coherent imaging radar could be subjected to different digital processing to obtain either optimum Doppler performance or maximum resolution as required by different users. Nevertheless, some compromise of certain radar parameters would be necessary to meet conflicting requirements of different applications.

The attainment of compatibility between Doppler processing and certain other features of radar systems can create system constraints, which are as follows:

Pulse compression: Doppler processing is fully compatible with pulse compression; but, with FM chirps, there are range errors proportional to Doppler; and, with other forms of code, there are increased range side-lobe levels caused by decorrelation effects from Doppler-shifted signals. Strong targets in range side lobes can contaminate the Doppler spectrum.

Multifrequency transmissions: Doppler processing may be applied simultaneously on multifrequency radars, but both the Doppler shifts and the blind speeds will be different at each frequency (for the same PRF).

Frequency agility: Doppler processing is not compatible with frequency agility unless steps are taken to transmit groups of pulses on each frequency, which also leads to a loss of signal pulses.

Synthetic aperture: The available coherent reference in this type radar may also be used for Doppler processing. There are errors in along-track range for moving targets because of the matched filter characteristics of the receiver.

Scanning beams: Doppler processing may be used with either mechanical or electronic beam scanning, but there is a broadening of the Doppler spectrum as a result of the movement (scanning) of the antenna beam. This broadening is generally significant only for very low Doppler speeds of high scan rates. The effect can be avoided with step scan, switched multiple beams, or Nyquist rate scanning.

Antenna null steering: Null steering in the directional pattern of the radar antenna may be used to reduce Doppler returns from

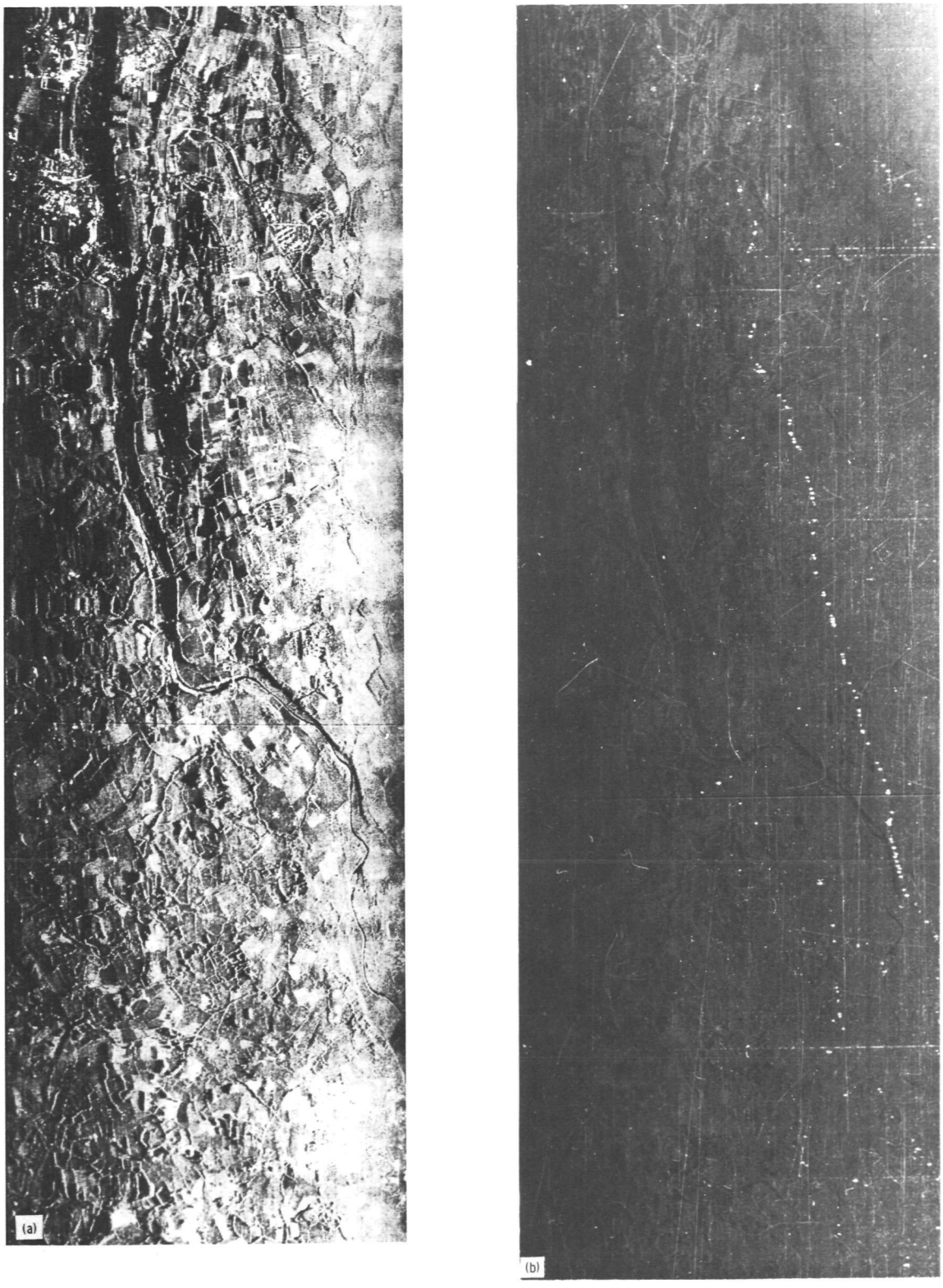

FIGURE 5–91.—Example of MTI. (*a*) Normal map. (*b*) Image with MTI processing.

c. 6

strong targets (such as the ground) where they mask wanted returns from precipitation. This technique is compatible with Doppler processing, but the null pattern should be constant over the integration time of the Doppler processing.

ANTENNAS AND ARRAYS

The current state of the art in antennas for spacecraft applications is discussed briefly in this section. A review of several of the more advanced antenna techniques is also included. These techniques are mostly used for ground radar installations and would require specialized development for spaceborne applications. The objective is to make users aware of the potential characteristics of such schemes because they are likely to be of increasing value for future systems.

Current State of the Art

Spacecraft have used parabolic reflection antennas 10 m in diameter in the Applications Technology Satellite (ATS) program. Using petals made of wire mesh hinged to a central hub, this antenna has a surface accuracy good to a 3-cm wavelength. This design is shown in figure 5–92. Antennas of these dimensions could also be produced for operation at millimeter wavelengths, which would probably require a continuous surface reflector or close mesh within a sandwich material.

Antennas with significant increases in diameter above 10 m would be more difficult to produce. One possible configuration is an inflatable balloon-type structure, but it is not clear whether this type antenna could maintain its tolerance with meteorite damage. Very large antennas could also encounter severe alinement problems, particularly related to heating from the Sun.

Antenna array systems.—During the past decade, new antenna techniques have been applied to radar systems. These techniques are based mainly on phased-array principles together with new developments in signal-processing technology and components. The antenna techniques include the following:

1. Electronic beam scanning.
2. The formation of multiple beams from a common aperture.
3. Placing and steering directional zeros in the antenna directional pattern.
4. Self-focusing and adaptive arrays.
5. Multiplicative processing arrays.
6. Arrays using separate patterns on transmit and receive to reduce the total number of elements.
7. Minimum-redundancy thin arrays.

Coherent synthetic aperture arrays should also be included in this list; however, they are discussed in more detail in other sections.

Electronic scanning and multiple beam forming.—Several relevant applications exist for electronic beam scanning for spaceborne radars where it is necessary to move the antenna beam at high rates or where it is convenient to use antenna array elements mounted over the surface of a given spacecraft (conformal arrays). Several phased arrays are now used on satellites.

The high cost of two-dimensional phased arrays for ground radars is caused by the need to handle very large power. In space applications, power levels are much less, and, for most instances, linear arrays incorporating one dimension of scan will be adequate. In some instances, the complication can be reduced by using array-thinning techniques, which are discussed later. Electronic scanning would not be relevant for very narrow beams from planar arrays because of the numerous elements.

An N-fold increase of data rate from a given radar-receiving aperture can be obtained by forming N separate independent beams from the aperture. This ability to make simultaneous measurements in multiple directions could have applications to scatterometers and narrow-beam sounders because it has the capability to increase resolution without loss of coverage or beam dwell time.

Multiple beams may be generated in a variety of ways, such as using multiple feeds

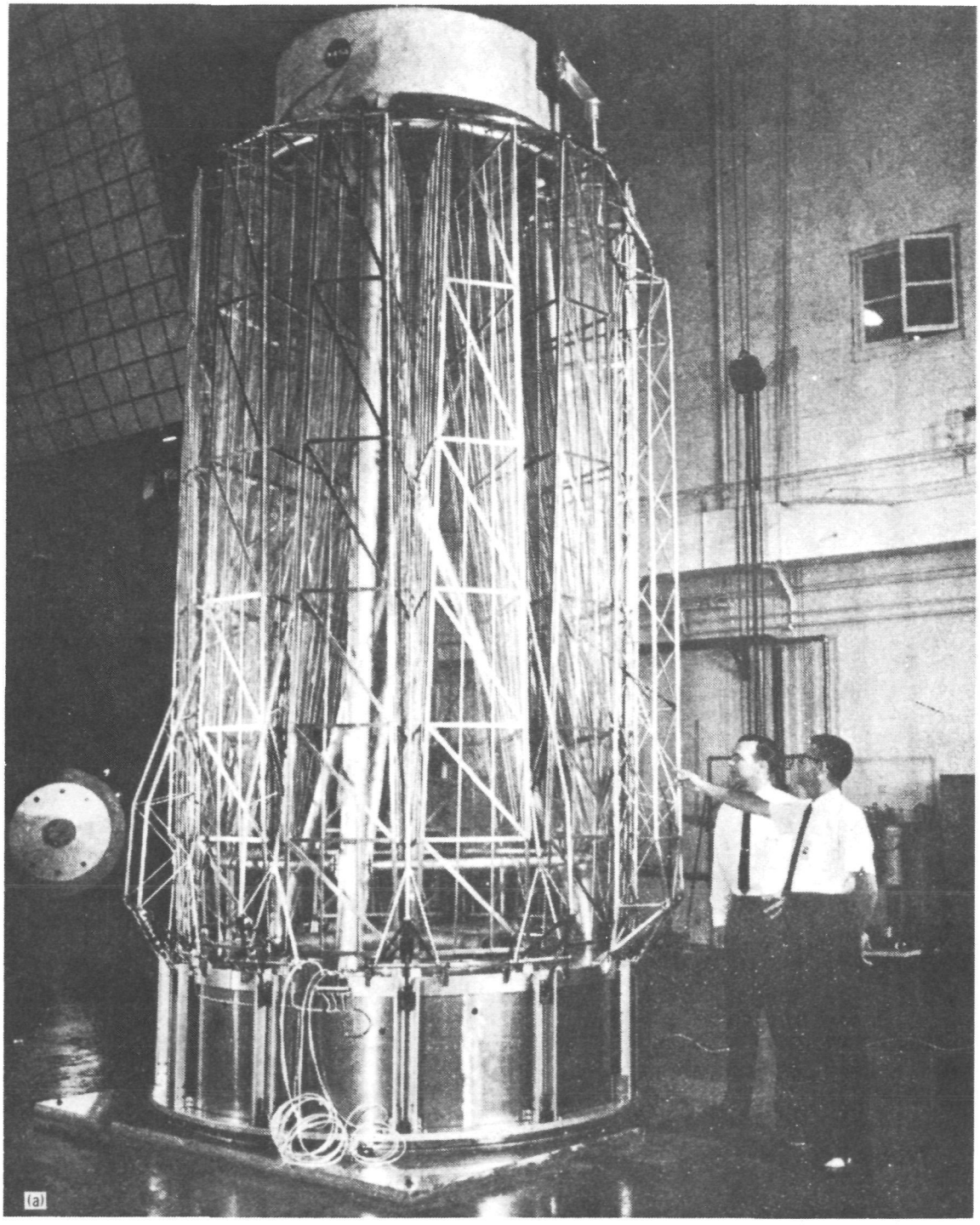

FIGURE 5–92.—Large space-erectable antenna reflector 9 m in diameter developed for the ATS program. The model has a paraboloidal structural design that can be collapsed for packaging into a launch-vehicle nosecone and then erected on command to its original shape. Each petal is permanently attached to its two adjacent petals before, during, and after erection. (*a*) Collapsed antenna.

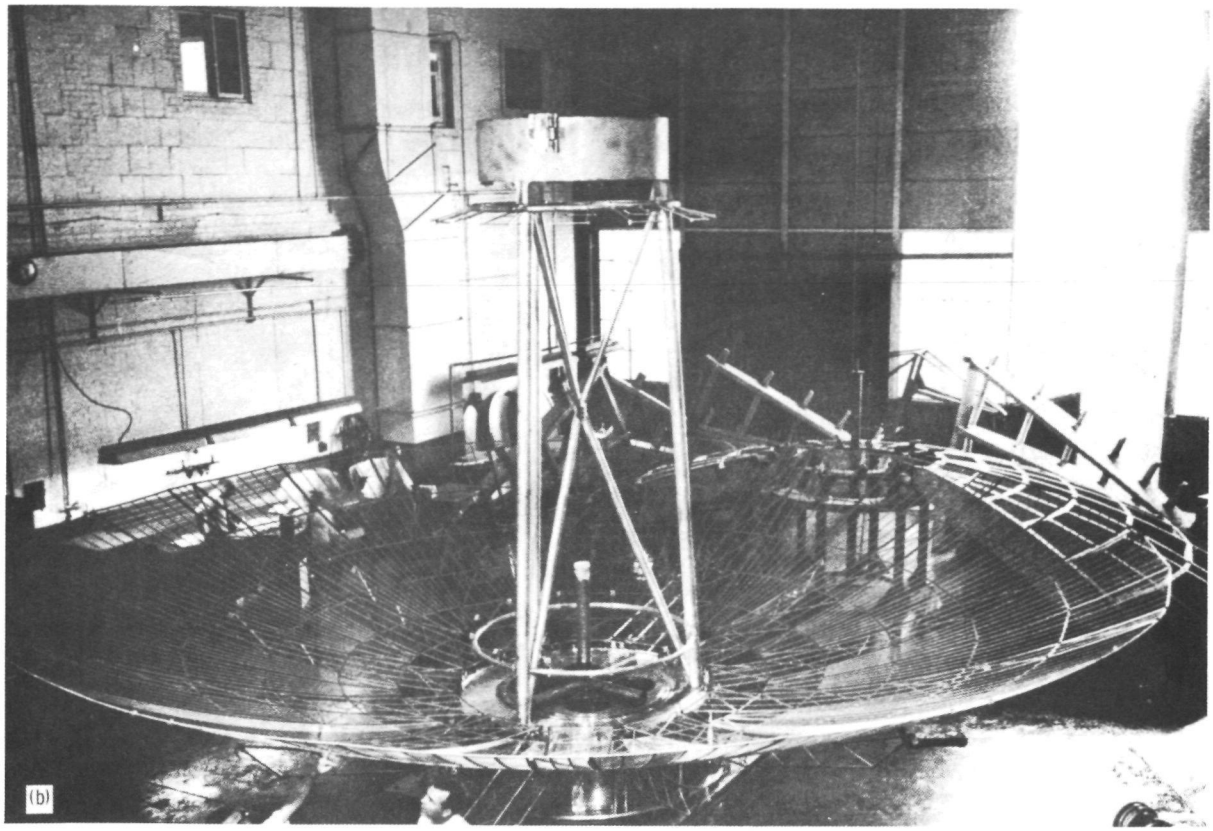

FIGURE 5–92 (concluded).—Large space-erectable antenna reflector 9 m in diameter developed for the ATS program. The model has a paraboloidal structural design that can be collapsed for packaging into a launch-vehicle nosecone and then erected on command to its original shape. Each petal is permanently attached to its two adjacent petals before, during, and after erection. (*b*) Erect antenna.

to parabolic or spherical reflections. Multiple-beam matrix networks, such as the Butler matrix network, can be used to generate independent beams from the output of antenna arrays. Monopulse tracking and zero steering can also be combined with multiple-beam matrix networks.

A group of high-data-rate radar systems is based on broad-beam (floodlight) transmission and either multiple-beam or Nyquist rate electronic beam scanning on reception. These systems offer very high angular data rates and derive their performance from more complex receiver processing, which benefits from the decreasing cost of digital velocity. An account of such radar systems using low-redundancy array techniques is discussed in the section entitled "Radar Systems Using Low-Redundancy Arrays."

Multiple beams may also be generated by digital FFT processing of the output of a receiving array, and synthetic aperture processing may be regarded as performing this technique in the Doppler domain.

Multiplication of directional patterns and thinned arrays.—Multiplicative arrays in which the output of array elements are demondulated by multiplying them in various combinations have been used for many years in radio-astronomy arrays. These arrays can provide incoherent antenna beams using the product of the signals from two crossed linear arrays (Mills cross). Work in this field has led to studies of large arrays

with low filling factors called minimum-redundancy arrays. The possible application of these arrays is discussed in more detail in the section entitled "Multiplicative Signal Processing."

Some radar applications described in earlier chapters need to use very large antennas in space. The requirement is often for very small beamwidths but without the need for high antenna gain. In such instances, it appears worthwhile to consider schemes that offer pencil beams generated from two crossed linear arrays, which might be technically easier to implement.

The Mills cross-type multiplicative beam applies only to reception. An alternative is to transmit using one linear array and to receive using the other array, thus forming a two-way pencil beam from the spatial product of the patterns. In this instance, there is a loss of transmitter power in the volume of the transmitter beam outside the common pencil-beam volume. If required, this loss of power may be removed by forming a set of multiple fan beams with the linear receiving array.

Adaptive arrays and zero steering.—Adaptive arrays control some aspect of the directional performance of the array to optimize some aspect of the received signal (using some automatic optimization process). The "self-phasing" performance is sometimes conducted by using separate pilot frequencies. Such arrays have had more application in communications than in radar.

Zero steering (null steering) arrays control the angular location of directional nulls in the antenna pattern to avoid illuminating and receiving signals from a specified direction, generally to avoid receiving some unwanted signals. This aspect of the system may be made adaptive. A possible application for such a system for spaceborne radar is the use of steered nulls to reduce Doppler clutter from ground returns. In such instances, it is possible to use a directional null to insert a corresponding null into the unwanted Doppler clutter spectrum. This effect can improve the capability of the radar to see returns from moving precipitation at the Doppler frequency of this null. The section entitled "The Extension of Meteorological Satellite Radar Coverage by Antenna Null Steering" gives a more detailed account of the use of null steering for improving Doppler performance.

The Application of Nonredundant Arrays to RAR and SAR Systems

Nonredundant arrays are linear (or planar) thinned arrays that are used in radio astronomy to synthesize the directional properties of filled receiving apertures. This section discusses how such techniques may be applied to radar systems to reduce substantially the number of antenna array elements. A particularly convenient radar-system configuration involves combining nonredundant arrays with within-pulse scanning of a receiving beam together with either frequency-agile transmissions or Doppler processing on reception to reduce effects of unwanted target cross products in the demodulation process. Schemes with square-law detection and multiplicative processing are discussed.

The application of such techniques to coherent SAR systems to reduce the amount of storage and processing of data needed for such systems is discussed.

Nonredundant arrays.—Nonredundant or partly filled arrays are used to a significant extent in radio astronomy but have found little application in radar systems. This section discusses several radar systems in which nonredundant and multiplicative arrays can provide significant reduction in the number of elements in the field of phased arrays for certain radar applications.

Aperture synthesis techniques have been used for coherent processing (i.e., for synthetic aperture side-looking radar) and for noncoherent receive-only applications (such as radio astronomy). For noncoherent applications, the synthesis procedure uses the fact that the cross-product signals from a pair of elements spaced a distance D apart in

a linear array is independent of the location of the elements in the array (provided the spacing D is maintained). The demodulated output of all receiving arrays consists of various weighted combinations of self-products and cross products of all element outputs; therefore, a substantial economy of elements (and associated processing) is possible if the duplication of any interelement spacing in the array can be avoided. Figure 5–93 shows a four-element array that contains all the interelement spacings from $D=1$ to $D=6$. This is a well-known example of a nonredundant array that contains all the spatial frequency components of a uniform seven-element array (ref. 5–31).

The conventional additive directional pattern of the array of figure 5–93 is most unattractive, having very high side-lobe levels, but the directional pattern of the output of the array after square-law detection is

$$D(p) = \frac{\sin(7p)}{\sin p} \qquad (5\text{–}43)$$

where $P = (\pi d)/\lambda \sin\theta$. This is the form of the normal pattern of a seven-element array. A conventional filled linear array involves a substantial duplication of element spacings. In most instances, it is difficult to produce arrays with each spacing occurring only once; thus, a compromise situation with a limited amount of duplication is acceptable. Low-redundancy arrays are the result of such a compromise.

Two reasons why such arrays have not found significant application in radar systems are as follows:

1. The radiated pattern from such arrays is unattractive because of very high side lobes. This can result in large amounts of the transmitted power residing outside the main beam.

2. The assumption that the cross product from a pair of elements (of fixed spacing) is independent of their location in the array is true only for incoherent signals (such as radio astronomy).

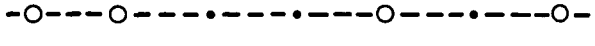

FIGURE 5–93.—Four-element array containing all the interelement spacings of a seven-element filled linear array.

Because there is no direct equivalent of nonlinear receiver signal processing for transmission, nonredundant arrays incorporating a low filling factor will exhibit high side lobes, which makes them unsuitable for transmission because of the significant loss of transmitter power. This problem can be overcome for radars incorporating floodlight transmissions together with either multiple beams or within-pulse scanning on reception. The widely spaced (low redundancy) arrays may then be used for the receiving array of such radars. A second area of potential application is coherent SAR, in which the minimum redundancy technique may offer a possible method for reducing the number of transmissions and associated storage required for the synthetic aperture process.

Radars incorporating floodlight transmitter coverage.—These forms of radar use phased-array techniques in conjunction with a floodlight transmitter. Figure 5–94 shows a sector illuminated by a floodlight transmitter, covered by a group of N fixed receiving beams. This type radar has the advantage of a very high data renewal rate. Figure

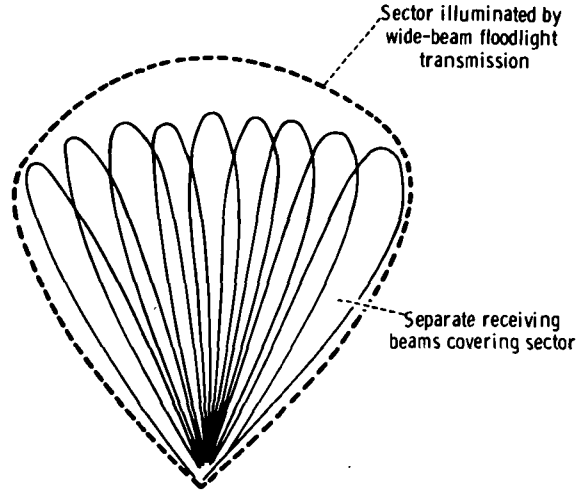

FIGURE 5–94.—Sector coverage by floodlight transmission and multiple-beam reception.

5–94 shows that both range and bearing are obtained on all targets within the coverage sector of the radar for each pulse repetition period.

The range performance of such a radar need not be significantly worsened by the use of floodlight transmissions. Although the radar range equation (as normally quoted) indicates that the maximum range is a function of the transmitting antenna gain, it is evident that the time average distribution of transmitting power is, for most conventional radars, uniform over the arcs of cover.

Comparing the radar configuration of figure 5–94 using a static floodlight coverage of a sector with the sequential illumination of each direction with a narrow antenna beam, it is clear that, in the former instance, data are obtained at a far higher renewal rate, but N times the number of pulses on each target are received, each containing $1/N$ of the energy (where N is the number of beam positions within the sector). The effect of such a system on maximum range performance is mainly dependent on the capability of the radar system to integrate these pulses, and this integration depends on target and noise statistics. In coherent integration, no loss of signal power would occur; but, for the more usual situation of incoherent integration, some reduction in maximum range would generally occur because of the less efficient integration. Therefore, such a radar will generally incorporate larger amounts of incoherent integration.

Various methods exist for generating such multiple beams, including multiple feeds to reflector or lens systems, special networks such as the Butler matrix, or sampling the outputs of the array followed by angular matched filters, such as digital FFT filtering. The third technique appears more suitable for the application of low-redundancy arrays by selecting the sampling points and processing to achieve the required array spacings. However, the application of low-redundancy arrays to radar can be conveniently described with reference to within-pulse scanning (ref. 5–32), which is another technique for receiving all the information on range and bearing from within an illuminated sector during a single pulse repetition interval.

Within-pulse scanning.—In this technique, a sector is illuminated with a floodlight transmission incorporating a pulse of duration τ, and a narrow receiving beam is scanned repetitively across this sector at a rate corresponding to $1/\tau$. Therefore, the scanning rate corresponds to the Shannon sampling rate or Nyquist rate, which means that pulses reflected from each target will be sampled by the scanning receiving beam, which effectively operates as a sampling switch for each direction. The technique is in operational use in the sonar field, but the radar application has been restricted to experimental devices (refs. 5–32 and 5–33).

Several alternative system configurations exist for providing Nyquist rate scanning of a receiving beam. The most well-known configuration is shown in figure 5–95. The output of each array element is subjected to single-sideband modulation at frequencies of ω_s, $2\omega_s$, $3\omega_s$, $4\omega_s$ . . . , where ω_s is the beam-scanning rate and equals $2\pi/\tau$. Such a scheme effectively adds a phase shift at uniform rates to each antenna element, thus producing a uniform movement of the array directional pattern along the sin θ scale. Each diffraction maximum of this pattern represents a beam that scans across the sector.

The noise factor of such a receiver is identical to that of a corresponding conventional receiving array provided that the

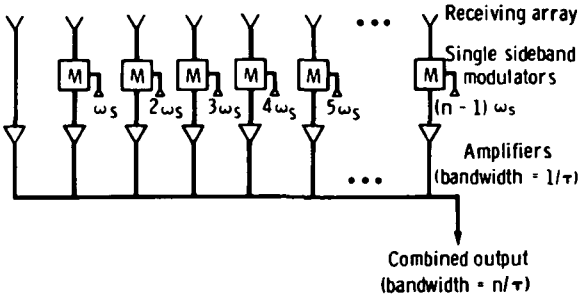

FIGURE 5–95.—Modulation scanning system to produce repetitive scanning of receiving beam at rate of ω_s ($\omega_s = 2\pi/\tau$).

bandwidth of the filters or amplifiers in each channel is restricted to $1/\tau$. However, although the bandwidth in each channel is $1/\tau$, the total bandwidth after summation of the channel outputs becomes n/τ (where n is number of channels), corresponding to the bandwidth of the sampled pulses (duration τ/n). Thus, the output represents the signals from N separate directions in space, which corresponds to the N-fold increase in bandwidth. The maximum range performance is not affected by the sampling process and corresponds to the previous examples of floodlight transmission.

The range resolution is determined by the transmitted pulse duration τ, and the side-lobe performance is set by one-way side lobes of the receiving array. A useful feature of the scanning receiver is that array amplitude tapers may be achieved by a single filter situated at the output of the combined array.

The MTI may also be applied to such a radar, and there is no reduction in performance due to scanning modulation, provided the pulse repetition interval is any integral multiple of the scan period.

Radar systems incorporating low-redundancy arrays.—Figure 5–96 shows the within-pulse scanning principle applied to the minimum-redundancy array of figure 5–90. The number of signal-processing channels is reduced in proportion to the number of elements in the array. Figure 5–95 also shows the frequency spectrum of such a scanning receiver when receiving a pure CW signal before and after detection. Before detection, there is a frequency component for each element of the thinned array. After square-law detection (at location X_2 in fig. 5–96), the "filled" spectrum corresponding to a seven-element array is produced.

The frequency spectrum of the output of a receiving array undergoing continuous scanning is a direct replica of the spatial frequency response of the array and associated signal processing. Figures 5–90 and 5–96 show how the square-law detection process produces a uniform filled spectrum giving the

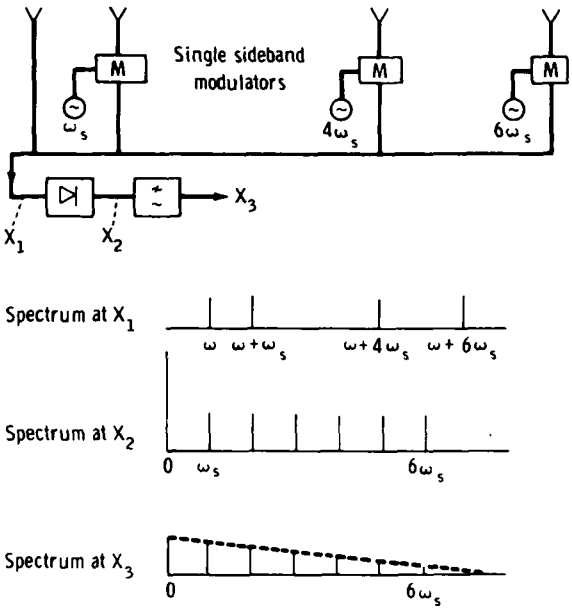

FIGURE 5–96.—Continuous electronic scanning of a nonredundant four-element array providing the directional pattern after demodulation of a filled seven-element array.

spatial frequency response of a filled array. However, because this spectrum corresponds to a $(\sin 7p)/(\sin p)$ power response, the side-lobe level would be too high for any radar application and would therefore require the application of amplitude tapers.

The adoption of the within-pulse scanning receiving system considerably simplifies such a tapering process. The capability for any side-lobe reduction technique appears to be determined by the range of possible amplitude tapers that could be applied to the thinned array. The well-known taper functions are not applicable to such nonuniformly spaced thin arrays. However, the output of the square-law detection enables separate access to each spatial frequency component of the processed pattern. Therefore, conventional taper theory can be applied at this point in the array processing. Apart from this additional degree of freedom in synthesizing the low side-lobe pattern, this technique has the additional advantages of enabling the taper to be applied after amplification and, hence, after the signal-to-noise

ratio has been defined. Another valuable feature is that, for many instances, the tapering function may be introduced by including a single filter at the output stage.

Figure 5–96 shows a simple low-pass filter included after detection to provide a triangular spectrum of spatial frequencies. This corresponds to a power response directional pattern of the following form:

$$D(p) = \left| \frac{\sin (7p)}{7 \sin p} \right|^2 \qquad (5\text{–}44)$$

This expression corresponds to the same side-lobe level as a uniform filled untapered array. Clearly, other filter responses corresponding to various low side-lobe patterns may be obtained by appropriate design of filters. The gain of such a thinned array is obviously reduced in proportion to the filling factor. The application of amplitude tapers causes the usual reduction of directivity (because of the slight increase of beamwidth).

The number of elements m in most low-redundancy array configurations is approximately given by $m=2\sqrt{n}$, where n is the number of element positions in a uniform filled array of the same dimensions. This fact means that the potential savings in elements and associated signal processing are most significant for large arrays and, particularly, for two-dimensional arrays used in radio astronomy. The significance of the reduction in gain greatly depends on the type of application for the radar.

Figure 5–96 illustrates the use of low-redundancy arrays for radar, but this particular example is of limited interest because it simulates a rather small array (seven elements) using four elements. Before considering designs for larger arrays and the use of other forms of demodulation, it is necessary to examine the multiple-target response of low-redundancy arrays and the effect of the coherence of the returns from targets.

Resolution and coherence.—If a directional receiver having a directional pattern $D(p)$ is illuminated by a source (or reflected signal from a target) of strength A_1 with frequency ω and direction θ_1, the receiver output will be

$$E_s = A_1 D(p_1) \cos (\omega t + \phi_1) \qquad (5\text{–}45)$$

where ϕ_1 is a general phase angle and $p_1 = (\pi d/\lambda) \sin \theta_1$. If this signal is square-law-detected and low-pass-filtered, the output will be proportional to

$$E_s = \frac{1}{2} A_1^2 D^2(p_1) \qquad (5\text{–}46)$$

A similar output would occur for separate excitation of the receiving array with a source A_2 at angle θ_2. However, for simultaneous excitation of the directional receiver, with both signals, the output after square-law detection and filtering becomes

$$E_s = \frac{1}{2} A_1^2 D^2(p_1) + \frac{1}{2} A_2^2 D^2(p_2) + A_1 A_2 D(p_1) D(p_2) \cos (\phi_1 - \phi_2) \qquad (5\text{–}47)$$

The first two terms are the outputs that would be predicted by superposition, and the third term is the cross product between two sources or targets.

Note that this cross-product term exists for all forms of directional receiver (whether using continuous apertures, filled arrays, or thinned arrays) and for all forms of demodulation. This cross-product term is an unwanted distortion, which reduces the ability to resolve multiple targets; thus, it needs to be reduced (ideally to side-lobe levels) relative to the wanted target self-products. Cross products between the signals from different element positions are the essential feature of a directional receiver; it is the cross product between different targets that must be removed (ref. 5–34).

For filled arrays with low side lobes, the target cross-product term is reduced because of the product $D(p_1) D(p_2)$. This fact shows that such cross products would be reduced to side-lobe levels if the angle between the two sources is greater than approximately one beamwidth.

Such target cross products fall off according to the autocorrelation of the predemodu-

lated directional pattern. Filled apertures use this property to reduce such effects. The amplitude of the target cross products is proportional to cos $(\phi_1-\phi_2)$, which represents the difference in phase of the returns from the targets A_1 and A_2. The phase difference will be random, which results in an average value of zero for the target cross product when averaged over all possible target positions.

For radio astronomy, the signals from two different radio sources are uncorrelated so that all such target cross-product terms average to zero, which explains the extensive use of thinned arrays in radio astronomy. However, for a radar system in which both targets may be illuminated from the same transmission, it may be necessary to introduce some deliberate variation of $(\phi_1-\phi_2)$ plus some averaging (integration) to integrate out the target cross products when a low-redundancy array is used.

The three principal methods for varying $(\phi_1-\phi_2)$ to achieve such results are as follows:

1. Movement of array: If the array moves relative to the target environment, the ranges (and hence the relative ranges) of the targets will change. To decorrelate returns from different targets by this method, it is necessary to obtain changes in $(\phi_1-\phi_2)$ in the region of one wavelength. Several such decorrelated responses must be averaged. Apart from the change of range, scintillation effects will occur because of complex targets, and changes of amplitude and phase returns will occur because of small changes of aspect angle. These effects will also help decorrelate the target cross-product returns.

2. Movement of targets: If the radar is used to obtain data on moving targets (using an MTI (or pulse Doppler) technique), Doppler filtering must be applied before detection. This technique necessarily removes most of the target cross products; it removes cross products between fixed targets and between moving and fixed targets, which leaves only cross products between moving targets. These cross products between moving targets will average to zero because of their relative movement. Thus, the unwanted cross products can be substantially reduced by the application of Doppler filtering followed by postdetector integration. The absence of scanning modulation effects for within-pulse scanning radars makes them particularly appropriate for MTI processing for certain applications, especially those involving very low speed targets.

3. Frequency agility: Changes in transmission frequency cause corresponding changes in the two-way phase delay to and from the targets and, hence, cause a change to $(\phi_1-\phi_2)$. Consequently, either multiple-frequency or frequency-agile transmissions for a radar incorporating low-redundancy arrays will enable the target cross-product returns to be decorrelated between successive pulses radiated at different frequencies. For distributed targets or clutter, it is generally necessary to change the transmission by an amount proportional to the transmitting bandwidth to decorrelate target returns from pulse to pulse. The technique of using frequency agility to reduce target cross-product effects has been demonstrated by Shearman et al. (ref. 5–35).

These three methods of reducing target cross products depend on noncoherent integration to average out the decorrelated returns. The extent of such integration will depend on the amount of decorrelation obtainable with the different methods and the degree of suppression of target cross products required. The level of cross products is proportional to the number of targets seen by the predemodulated directional pattern. The required integration is therefore substantially reduced for a thin target field (e.g., moving targets only). The only method not requiring integration is the filled aperture, which can be regarded as coherent integration of cross products within the array. The combination of low-redundancy arrays with within-pulse scanning is particularly convenient because the within-pulse scanning system requires the use of noncoherent in-

tegration for other purposes as previously discussed.

The unwanted effects of target cross products are not absent in filled arrays. Although there is considerable duplication of close element spacings, the relative weighting of element spacings in the spatial response of the array is triangular with no duplication of the largest spacing. This results in target cross products affecting the resolution of targets when closely spaced (within approximately two beamwidths of each other). For a nonredundant array, this effect can occur for all possible target directions.

Multiplicative signal processing.—The minimum-redundancy arrays discussed in the preceding section depend on the nonlinear performance of the demodulation process for their performance. In practice, all radar systems incorporate some form of nonlinear demodulation, but the effect on resolution performance is not very significant for filled arrays.

The use of multiplicative signal processing to demodulate the signals from directional arrays is an alternative form of nonlinear demodulations, which has been studied by many authors (refs. 5–34 and 5–35), and is used extensively in radio astronomy for noncoherent aperture synthesis and for synthesizing two-dimensional apertures from line arrays such as the Mills cross system (ref. 5–36).

Figure 5–97 shows how the directional pattern of a 36-element filled array can be obtained by multiplying the patterns of a 6-element wide-spaced array with a second 6-element closely spaced array. The array pattern multiplication theorem states that the overall directional pattern of an array is the product of the array factor and the directional pattern of each element. In figure 5–97, the short filled array is used as a single directional element, which is multiplied by the output of the wide-spaced array to synthesize a filled array of 36 elements.

No difference of principle exists between the adoption of square-law detection systems, such as those in figure 5–96, and the multiplication systems. Both techniques produce different combinations of self-products and cross products between signals from array elements. For example, a multiplier can be synthesized from three hybrids and two square-law detectors.

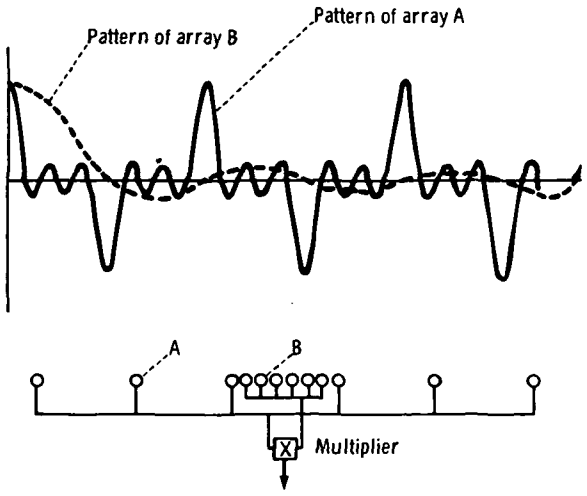

FIGURE 5–97.—Directional pattern of filled array produced by multiplying the output of the short filled array with the output of the wide-spaced array.

The scheme of figure 5–97 can be subjected to electronic scanning (for receive only) by appropriate phasing of the short and long arrays. There is a substantial economy of elements, phase shifters, and associated signal-processing equipment because the m_1 elements in the first array and the m_2 elements in the second array synthesize the directional pattern of an n-element linear array

$$D(p) = \frac{\sin np}{n \sin p} \qquad (5\text{–}48)$$

where $n = m_1 m_2$. This pattern is a power-law response; therefore, amplitude tapering would be necessary to achieve good side lobes.

The economy of elements increases with the size of the array; only 20 elements are needed for a 100-element-position array (20 percent filling) and only 68 elements for a 1000-element-position array (20 percent filling). Many configurations also exist for synthesizing planar arrays such as the Mills cross array (ref. 5–35), which produces an n-element planar array from two linear ar-

rays of m_1 and m_2 elements (again $n = m_1 m_2$).

Figure 5–98 shows a schematic diagram of a within-pulse scanning radar for such an array configuration. The long and short arrays are shown physically separated for convenience, but the arrangement of figure 5–97 would probably be chosen. The radar incorporates frequency agility and video integration to suppress cross products. The frequency agility is removed at each receiving channel of the radar before narrowband amplification and modulation to achieve the continuous electronic scanning process. Multiplication of the outputs of the two arrays is conducted in the intermediate-frequency section.

A further valuable feature of the multiplicative array configuration of figures 5–97 and 5–98 is that, because most element spacings are already repeated in the two basic arrays, a substantial reduction of cross products occurs before demodulation.

Applications.—The usual applications for either within-pulse scanning or multiple-beam systems incorporating floodlight transmissions involve high data rate coverage of a fixed sector. For applications to aircraft or spacecraft, this tends to suggest fore or aft surveillance for those situations in which conventional scanning might be inconvenient, when the data rate might be too low, or when the presence of scanning modulation might degrade the required Doppler performance. The within-pulse scanning-type system does not appear relevant to side-looking applications because the equivalence of bearing information is obtained by along-track movement of the craft.

Possible alternative applications of such systems include the provision of radar altimeter information over a wide arc of cover-

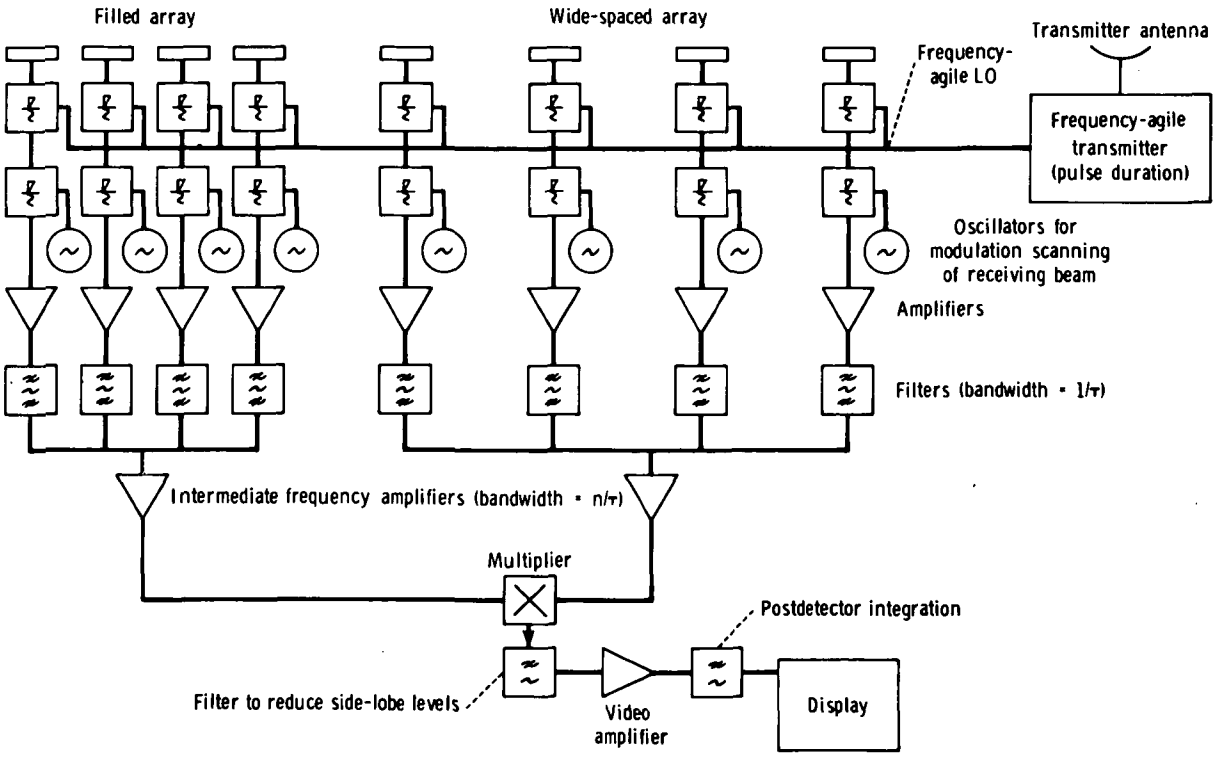

FIGURE 5–98.—Multiplicative array with within-pulse scanning on reception. Filled array containing m_1 elements multiplied by wide-spaced array containing m_2 elements to synthesize filled array with $n = m_1 m_2$ elements.

age below the craft; a further alternative might include scatterometer measurements over a similar wide arc. When the use of narrow fan beams or pencil beams is deemed advantageous, the previously discussed use of low-redundancy arrays offers substantial economies in numbers of elements required for the arrays and associated economies in processing circuitry.

Application of low-redundancy arrays to SAR.—The previous sections have been concerned with the application of low-redundancy arrays to the receiving aperture phased arrays for radar. This section concerns the possibility of extending the concept to synthetic aperture coherent radars with the objective of a significant reduction in the large amounts of data storage needed for such radars, particularly when using digital signal processing. The proposals are tentative and are meant to justify a more detailed study to establish the probable advantages for practical radar configurations.

The SAR uses phase-coherent transmissions (usually pulses). By storing and processing the received signals for many pulses, an equivalent two-way directional pattern of a long linear array can be synthesized. Details of such radars have been described in considerable detail in other sections.

The possible application of nonredundant arrays to the far-field patterns of the unfocused synthetic aperture is considered because this is a convenient direct extension of the far-field concepts of previous sections. However, the arguments also apply, with little modification, to focused arrays. The processed and filtered output of the radar is a signal that relates to a synthetic array in which each element position is the position of the physical array at the time of each transmission/reception. This processed output must be demodulated, and, as with the real arrays discussed previously, the detection process generates cross products between all possible pairs of element positions in the synthetic aperture. Again, there are substantial redundancies in such cross products, which suggest that it should be possible to reduce the number of transmission/reception positions in a given synthetic array length. This reduction would lead to some nonfilled pattern of transmission and reception positions within the synthetic array length, thus leading to a corresponding reduction of storage and processing.

Consider the original minimum redundancy array of figure 5–96. If an SAR moved along the line of this array transmitting and receiving only at the positions of the four elements, the output of the processor could be square-law-detected to provide the same postdemodulation directional pattern that would have resulted (before detection) from transmitting and receiving at all seven positions. This fact is certainly valid for the case of single-target directional patterns; the effect of coherence and unwanted multiple-target cross products will be discussed later.

The multiplicative scheme of figure 5–97 can also be translated into the synthetic aperture field. In this case, the radar would transmit and receive at the positions of the wide-spaced array and process this to produce the directional pattern of a synthetic array with wide element spacing. The resultant directional pattern would have angular diffraction lobes of the same form shown in figure 5–97. If the radar also transmitted and received at the locations of the shorter array, these outputs could be similarly processed to produce the synthetic pattern of a short filled array. The outputs of these two processed patterns can therefore be multiplied to produce a demodulated output having no diffraction lobes.

For such a scheme, the resolution of a synthetic aperture of n-element positions can be achieved by transmitting and receiving at m_1 and m_2 positions (where $n=m_1m_2$). This obviously represents a potentially valuable saving in storage and data processing. There is a loss of range performance as a result of the reduction of mean transmitted power by the same ratio. This loss can be recovered in principle by a corresponding

increase of peak transmitter power at those positions where the radar is activated.

A conventional SAR processes the output of the last n-pulse repetition intervals each time the physical aperture moves its own length. This is not possible with the previously mentioned two schemes, because the low-redundancy array configurations are not a continuous uniform series. For these cases, it is only possible to synthesize the required pattern at the end of the particular array pattern. To avoid gaps in the radar cover, it is also necessary to produce a processed output from the radar once for every position of the filled synthetic array. Figure 5–99 shows a different configuration of multiplicative array. The outputs of two thinned arrays having the same overall length but containing five and six elements, respectively, are multiplied. This figure shows that the resultant multiplicative pattern removes the diffraction lobes of the two constituent arrays. This resultant directional pattern is derived from 9-element positions and has a beamwidth and side-lobe level similar to the one-way pattern of a 21-element array (considering the power-law response).

The advantage of this configuration is that the output of the previous 9-element positions can be used to form such a pattern by synthetic aperture processing. However, this configuration does not solve the problem of deriving processed outputs from the radar for those positions of the real array at which there are no transmission and reception. This problem can be solved by tak-

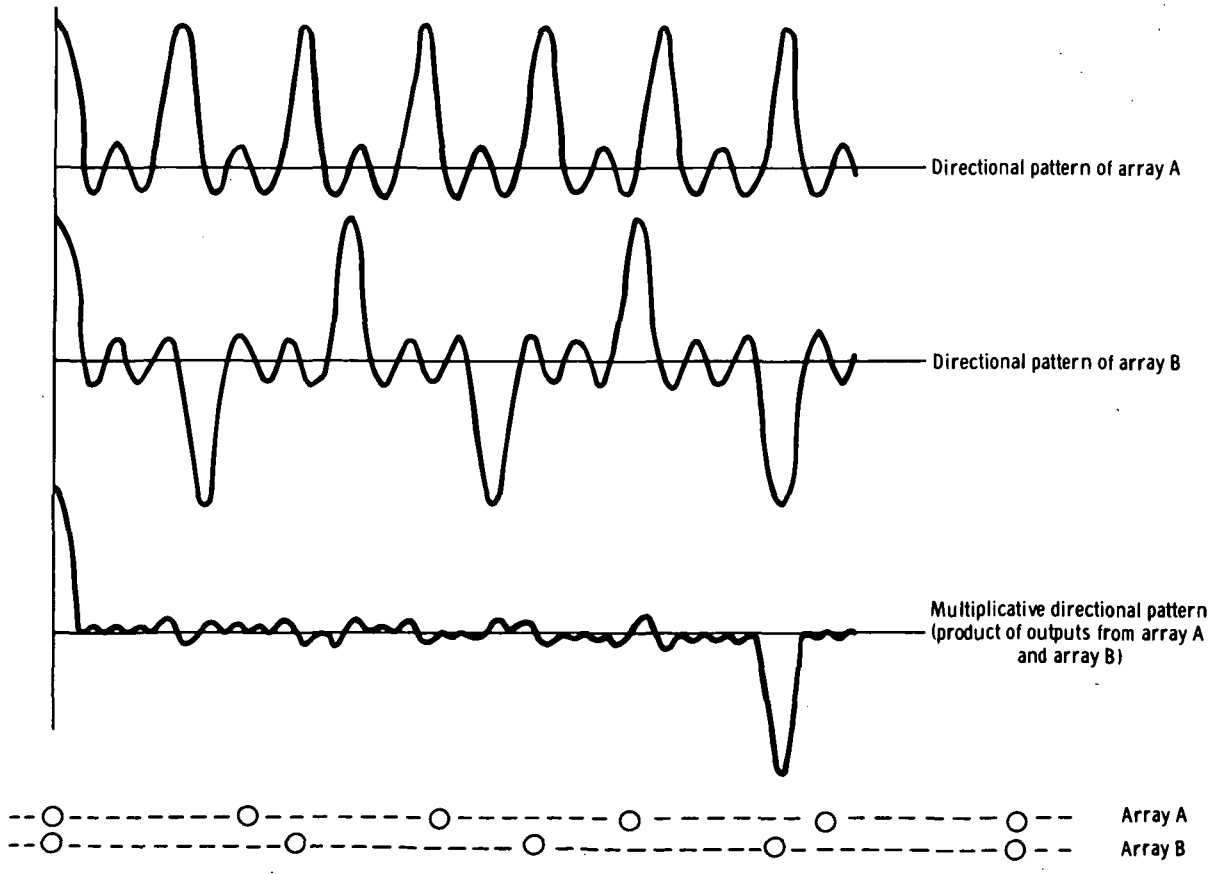

FIGURE 5–99.—Multiplicative product of outputs of two wide-spaced arrays that have the same total length but different numbers of elements.

ing the stored outputs from the active element positions and by processing these with different phase shifts to synthesize the beam outputs for the missing element positions.

It is also possible to apply this type technique to produce a continuous data output for the previous multiplicative configuration of figure 5–97. In this case, because the short filled array position is activated only infrequently, the resulting synthetic directional pattern changes slightly as the radar moves.

Because an SAR depends on some degree of coherence between the returns from each target over several transmissions throughout the length of the synthetic aperture, cross products between different targets will obviously arise. The methods of removing such target cross products, which were discussed earlier, will still apply in principle, but there are now rather different practical problems. For example, if frequency agility is used, it is still necessary to retain coherence over each synthetic aperture length so that the frequency-agile transmissions are interlaced with the other transmissions and the outputs added after demodulation. The obvious disadvantage of this approach is that it requires increased data storage in proportion to the number of different frequency transmissions per element position. Multifrequency transmissions with similar properties would be an alternative approach.

The most promising method of reducing cross-target products would probably be Doppler processing, but this restricts the applications to study of moving targets. In mapping areas of distributed targets (e.g., terrain), the level of cross products will be high.

For systems in which the low-redundancy array is used with SAR incorporating transmission to ground-based data processing, the telemetry bandwidth would be reduced. Nevertheless, it would be necessary to include some degree of buffering storage in the radar to smooth the flow of data.

Conclusions.—This section has shown how the nonredundant arrays used in radio astronomy may be used in radar applications for both RAR and SAR systems. Such schemes lead to an economy of elements in the array configuration in which typically $2\sqrt{n}$ elements are used to synthesize an n-element array; thus, the most significant savings are made for large arrays.

In the case of RAR, it is particularly convenient to combine low-redundancy arrays with within-pulse scanning. With such arrays, the demodulation process introduces target cross products that can be suppressed by using either frequency-agile transmission or Doppler filtering, followed by noncoherent integration. Such schemes offer attractive savings of array elements and associated processing for surveillance applications.

The application of low-redundancy arrays to SAR is more difficult to evaluate because it depends on the extent of target cross products for practical situations and their effect on the resultant radar maps. However, the potential storage savings should justify some further studies of these applications.

The Extension of Meteorological Satellite Radar Coverage by Antenna Null Steering

To use satellite-borne radar effectively for meteorological observations, ground clutter must not mask the returns from precipitation. A restriction is therefore imposed on the swath that can be covered by the satellite radar, because the range cell at extended crosstrack distances from the subsatellite point is inclined at an angle to the Earth, and returns from precipitation are masked by returns from the ground included in the cell (ref. 5–37). Narrowing the antenna beamwidth extends the crosstrack range. Also, MTI processing presents some promise for ground-clutter reduction, although this has been disputed. The backscatter from calm seas at low elevation angles may be sufficiently low to allow detection of moderate rainfall in the presence of sea clutter. However, over the land, clutter returns can be anticipated to be 5 to 25 dB stronger than returns from moderate rainfall.

The straightforward approach to avoid ground clutter by a meteorological satellite radar is to use an antenna beamwidth that is sufficiently narrow to minimize illumination of the Earth at the edge of the swath. Other considerations may restrict the antenna size below that needed for clutter reduction. This section outlines a method of ground-clutter reduction. The method consists of placing a null at the angle corresponding to the direction of the surface of the Earth at a given range. Techniques for accomplishing this task can vary from tilting a conventional antenna away from the Earth to controlling a null steering array. These techniques result in a gain reduction in the boresight direction.

The limitation on swath width.—A simple relationship exists between the satellite altitude, swath width, antenna beamwidth, and minimum detection height. A satellite is assumed to be at an altitude H above the Earth and to be detecting precipitation at a height h above the Earth at a crosstrack distance D from the subsatellite point (fig. 5–100). The radar pulse length is τ, which results in a range cell extent of $c\tau/2$. The boresight direction of the antenna is the direction of the precipitation target at height h, and the antenna pattern is assumed to have a null in the direction corresponding to the ground intercept point A. The angular width of the antenna pattern between the boresight and the first null is ϕ. For a conventional antenna, this is approximately equal to the half-power beamwidth. The relationships between the parameters shown in figure 5–100 are

$$h=r\cos\beta+\frac{c\tau}{2}\sin\beta \qquad (5\text{–}49)$$

$$(H+R_E)\sin\alpha=R_E\cos\beta \qquad (5\text{–}50)$$

$$r\sin\alpha=R_E\sin\theta \qquad (5\text{–}51)$$

$$D=R_E\theta \qquad (5\text{–}52)$$

leading to

$$h=r\phi\left(1+\frac{H}{R_E}\right)\sin\alpha+\frac{c\tau}{2}\sin\beta \qquad (5\text{–}53)$$

or

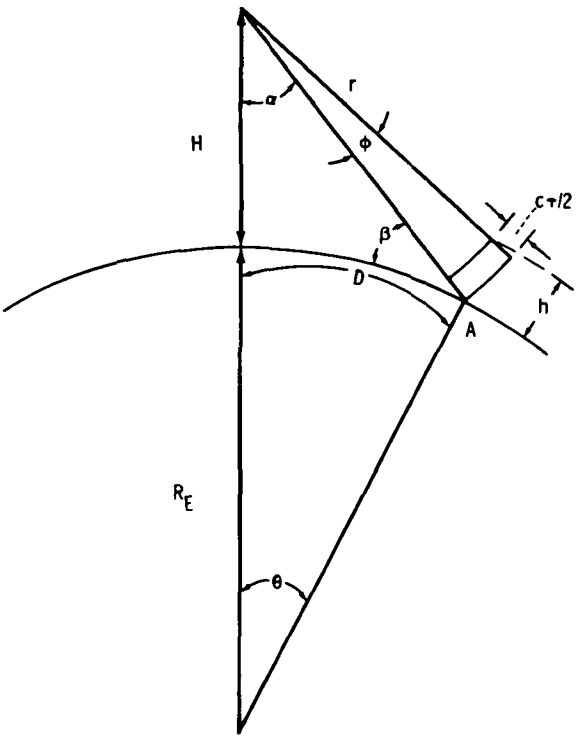

FIGURE 5–100.—Geometry describing the coverage of a satellite-borne radar.

$$h=D\phi\left(1+\frac{H}{R_E}\right)\left(\frac{\sin\theta}{\theta}\right)+\frac{c\tau}{2}\sin\beta \qquad (5\text{–}54)$$

If the radar pulse is short so that the range extent is small compared to h, the previous equation can be approximated by

$$h=D\phi\left(1+\frac{H}{R_E}\right) \qquad (5\text{–}55)$$

without incurring an error over 10 percent for the first 5000 km of crosstrack distance. The equation has been plotted for a range of parameters in figure 5–101. The crosstrack distance is greater for lower satellite altitudes.

The use of pattern nulls for clutter reduction.—Targets at heights below h will be masked by ground clutter because the antenna beam intercepts the Earth. However, if a pattern null were set at the direction of the ground intercept for a given range, the ground clutter would be substantially reduced.

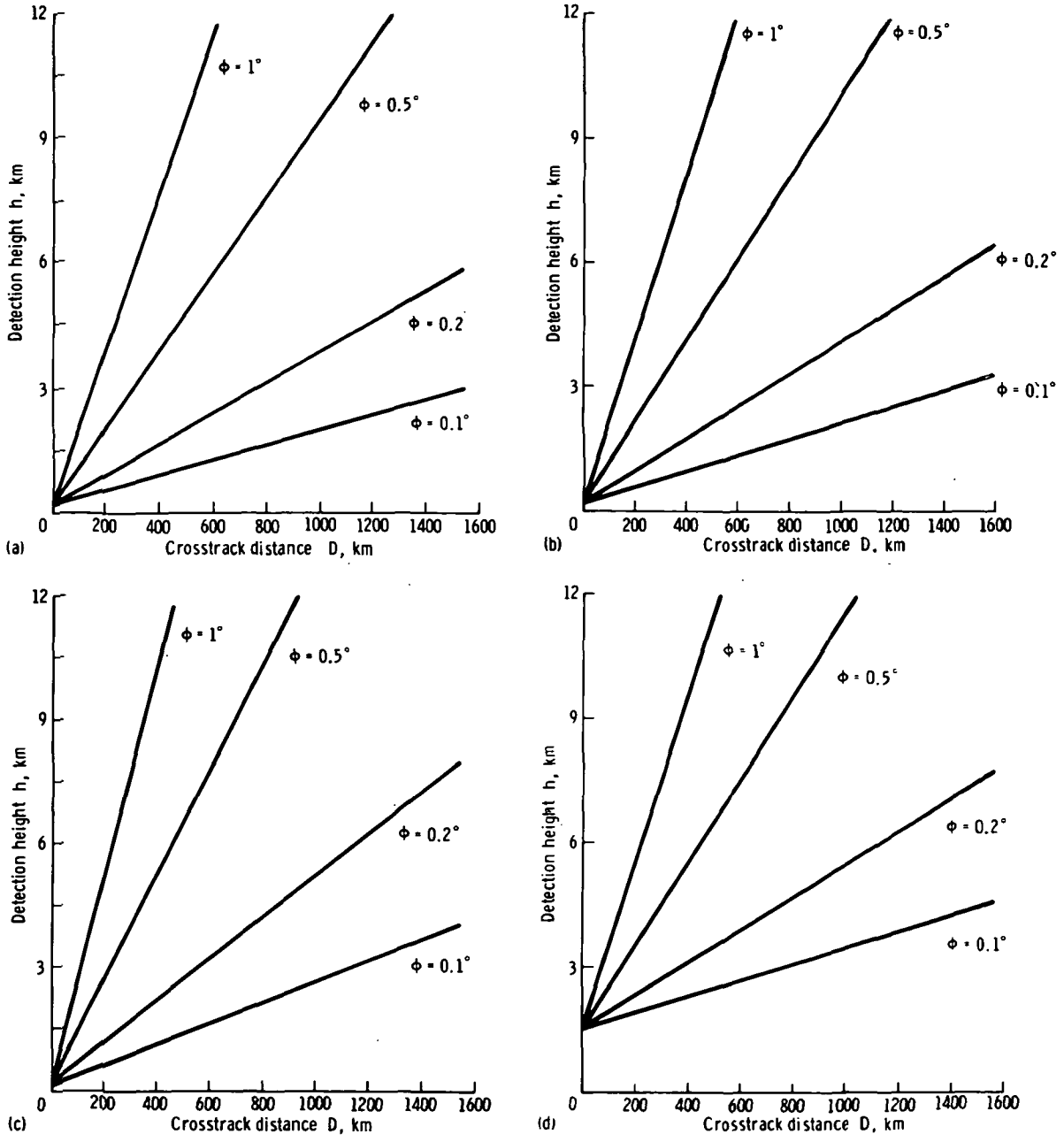

FIGURE 5–101.—Minimum detection height as a function of crosstrack distance for a range of parameters τ and H (ϕ=0.1°, 0.2°, 0.5°, and 1.0°). (*a*) H=322 km, τ=1 μsec. (*b*) H=965 km, τ=1 μsec. (*c*) H=2896 km, τ=1 μsec. (*d*) H=965 km, τ =10 μsec.

The nulls of the pattern of an array antenna can be positioned by the adjustment of the excitation coefficients of the array elements. The problem of maximizing the gain in a given direction while positioning a null at another direction has been studied by Drane and McIlvenna (ref. 5–38). The curve in figure 5–102 labeled "Null steering array"

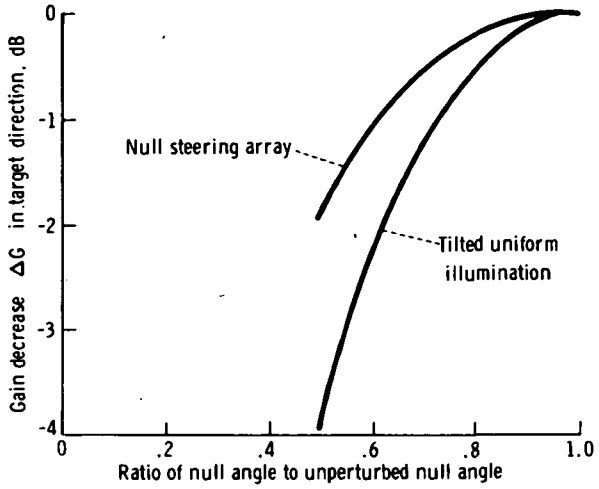

FIGURE 5–102.—Gain decrease in the target direction for null steered array and tilted uniform illumination.

shows the decrease in gain in the boresight direction as the null is steered into the main beam region. This figure illustrates that a null can be placed at an angle from boresight of one-half that of a conventional array, with an attendant reduction of 2 dB in one-way gain. This gain reduction would correspond to a lowering of radar sensitivity such that the minimum rainfall rate that could be detected would be increased by a factor of 1.78. Assuming that a 4-dB sensitivity margin could be built into the radar receiver, the ground swath width could be extended by a factor of 2 over that shown in figure 5–101.

Tilting the beam of a conventional antenna array away from the Earth will also achieve the desired result. However, the reduction in gain in the target direction is greater than that for a null steering array. The curve in figure 5–102 labeled "Tilted uniform illumination" shows the gain decrease as the antenna beam is pointed away and the null moves toward the ground intercept. For a tilt of one-half the peak-to-null angle, the gain in the target direction is lowered by approximately 4 dB, corresponding to an equivalent sensitivity to rainfall rates 3.4 times greater than that for the maximum gain direction.

The width of the null determines the number of range cells for which the ground clutter is effectively reduced. For the tilted antenna, the angular width of the null region for a clutter reduction of 26 dB, relative to the precipitation return direction, is 0.286 times the angle from the beam peak to the null. For the null steering array, the 26-dB clutter suppression zone is approximately 0.20 times the width of the unconstrained peak-to-null region. More than one null can be positioned near the ground-intercept direction to provide an extended region of clutter suppression.

Conclusions.—By steering the first null of the satellite antenna radiation pattern to coincide with the ground-intercept point, the crosstrack range of coverage of a meteorological satellite radar can be extended. Techniques exist for null steering by adjustment of the amplitude and phase of array excitation coefficients. As the null is steered into the main beam region, there is a directivity reduction. A simpler technique is to tilt the beam of a conventional antenna away from the Earth; however, this technique results in a larger gain decrease for a given null shift than for an optimized null steering array.

For example, consider a satellite at an altitude of 1000 km with an antenna beamwidth of 0.25°. At a wavelength of 0.8 cm, the crosstrack aperture size would be approximately 2 m. For a minimum detection altitude of 1.5 km, the maximum crosstrack distance from the subsatellite point would be 300 km. To cover ground ranges in excess of this distance, the null would be steered, extending the crosstrack distance to 650 km from the subpoint. The total swath width would be 1300 km, with an increase of 78 percent in the minimum detectable rainfall rate at the swath edges. The null steering must be linked to the range window so that the clutter-suppression zone corresponds to the desired set of range cells.